

# Dynamics of Internally Converted Electron-Positron Pairs\*

N. P. SAMIOS

Columbia University, New York, New York and Brookhaven National Laboratory, Upton, New York

(Received August 19, 1960)

The reactions studied were  $\pi^- + p \rightarrow n + \pi^0$  ( $\pi^0 \rightarrow \gamma + e^+ + e^-$ ) and  $\pi^- + p \rightarrow n + e^+ + e^-$ . From a sample of  $\sim 15\,000$  internally converted electron-positron pairs, 7000 were measured, of which 4200 were used in the detailed analysis. The differential distributions in  $y$  (the energy partition) and  $x^2$  (the virtual mass of the photon) agree with the theoretical quantum electrodynamic calculations. A measure of the form factor for the  $\pi^0 \rightarrow 2\gamma$  reaction gave a value  $\Gamma(x/\mu) = 1 - (0.24 \pm 0.16)x^2/\mu^2$ , where  $\mu$  is the mass of the pion. It was further demonstrated that the number of events necessary to determine the contribution of the longitudinally polarized virtual  $\gamma$  rays in the second reaction is of the order of 50 times that in the present experiment.

## I. INTRODUCTION

WHEN  $\pi^-$  mesons are captured at rest in hydrogen, the two most probable reactions which occur are:

$$(A) \pi^- + p \rightarrow n + \pi^0 \rightarrow 2\gamma,$$

$$(B) \pi^- + p \rightarrow n + \gamma.$$

In fact, the ratio of A to B is precisely the Panofsky ratio. It was first pointed out by Dalitz<sup>1</sup> that the  $\pi^0$  has an alternate decay mode, namely,

$$\pi^0 \rightarrow \gamma + e^+ + e^-,$$

where one of the  $\gamma$  rays is internally converted into an electron-positron pair (i.e., a Dalitz pair). This occurs with a probability  $\sim 1/160$  for a single  $\gamma$  ray or  $\sim 1/80$  for either  $\gamma$  from  $\pi^0$  decay. This process was observed first in emulsions<sup>2-4</sup> where each experimental group observed between 5-10 pairs; then by counter techniques<sup>5</sup> whereby the  $\gamma$  ray was detected in coincidence with an electron; and finally in cloud chambers<sup>6,7</sup> where in one case  $\pi^-$  mesons were stopped in the chamber, and in the other had a kinetic energy of 128 and 162 Mev, both experiments yielding of the order of 30 events.

Kroll and Wada<sup>8</sup> then proceeded to show that reaction (B) could also proceed via another channel; namely,

$$\pi^- + p \rightarrow n + e^+ + e^-,$$

where the  $\gamma$  ray from radiative capture is internally converted. Ten to fifteen examples of this process were

observed in the Columbia cloud chamber.<sup>6</sup> In all the above experiments, the yield of events was low. This resulted in large uncertainties in the experimental determination of the internal conversion coefficients with little or no opportunity for checking the details of the distributions predicted by the quantum electrodynamic calculations. With the advent of the hydrogen bubble chamber, it became possible to remedy this situation by accumulating a large number of events. In this experiment  $\sim 15\,000$  internal pairs were found of which 7000 were selected and measured. These events were then compared with the theoretical predictions as outlined by Dalitz,<sup>1</sup> Kroll and Wada,<sup>8</sup> and more recently Joseph<sup>9</sup> as far as the purely electromagnetic interactions were concerned, and with the predictions by Geffen and Berman<sup>10</sup> which concerned the strong interactions.

## II. EXPERIMENTAL DETAILS

The 60-Mev  $\pi^-$  beam at the Nevis cyclotron was slowed down by polyethylene absorbers and made to stop in a hydrogen bubble chamber. The chamber was cylindrical in shape, 12 in. in diameter and 6 in. in depth. It was placed in a magnetic field whose central value was 8.8 kgauss for approximately one-third of the pictures and 5.5 kgauss for the remaining two-thirds. The magnetic field was flat, dropping by 4% of its central value at the edges of the chamber. The central value of the field was controlled to  $\pm 2\%$  throughout the duration of the run. Details of the construction and operation of the chamber have been previously described.<sup>11</sup> A total of  $\sim 200\,000$  pictures were used in this analysis with  $\sim 10-15$  stopping  $\pi^-$ 's per picture. Figure 1 is a photograph of one of these pictures containing an electron-positron pair.

## III. SELECTION OF EVENTS

In order to insure sufficient accuracy in the measurement of each track, a fiducial region was chosen in the

\* This research is supported by the U. S. Atomic Energy Commission.

<sup>1</sup> R. H. Dalitz, Proc. Phys. Soc. (London) **A64**, 667 (1951).

<sup>2</sup> R. A. Daniel, J. H. Davies, J. H. Mulvey, and D. H. Perkins, Phil. Mag. **43**, 753 (1952).

<sup>3</sup> J. Lord, J. Fainberg, D. Haskin, and M. Schein, Phys. Rev. **87**, 538 (1952).

<sup>4</sup> B. M. Anand, Proc. Phys. Soc. (London) **A220**, 183 (1953).

<sup>5</sup> P. Lindenfeld, A. Sachs, and J. Steinberger, Phys. Rev. **89**, 531 (1953).

<sup>6</sup> C. P. Sargent, R. Cornelius, M. Rinehart, L. M. Lederman, and K. Rogers, Phys. Rev. **98**, 1349 (1955).

<sup>7</sup> Yu. A. Budagov, S. Wikton, V. P. Dzhelepov, P. F. Yermolov, and V. I. Moskalev, Dubna Report P-403, 1959 (unpublished).

<sup>8</sup> N. M. Kroll and W. Wada, Phys. Rev. **98**, 1355 (1955).

<sup>9</sup> D. W. Joseph, Nuovo cimento (to be published).

<sup>10</sup> S. M. Berman and D. A. Geffen (private communication).

<sup>11</sup> F. Eisler, R. Plano, N. Samios, M. Schwartz, and J. Steinberger, Nuovo cimento **5**, 1750 (1957).

plane of the chamber, and only events whose vertex fell within this region were measured. This region consisted of a circle concentric with the cross sectional area of the chamber but encompassing approximately half the area. This gave a minimum length of 4 cm per track and also reduced the number of usable events from 15 000 to 7000. Furthermore, only those electron-positron pairs were considered to be internally converted which had their origin within 1 mm of the  $\pi^-$  stopping. This insured catching all the internal pairs but introduced a contamination of  $\sim 8$  external pair events, as will be described later. A portion of the pictures were re-scanned by an independent observer and the efficiency for detecting events inside the fiducial region was found to be greater than 97%. Furthermore, these missed events were likely to come from either the charge exchange or the radiative capture reactions, so that no correction for these few events was made.

#### IV. MEASUREMENT

The electron-positron pairs were measured on a digitized scanning table with a precision of  $\sim 2$  microns on the film. The  $x, y$  coordinates of three points on each track, approximately equally spaced, were measured in each of three views (the vertex being the common point for both tracks) and the spatial information was computed on an IBM 650. The magnetic field in the chamber was measured by a proton resonance at the center and flip coil at all other points. This field distribution was fit by an equation constrained by Maxwell's equation. This expression was then used in the IBM program to compute the momentum of the tracks.

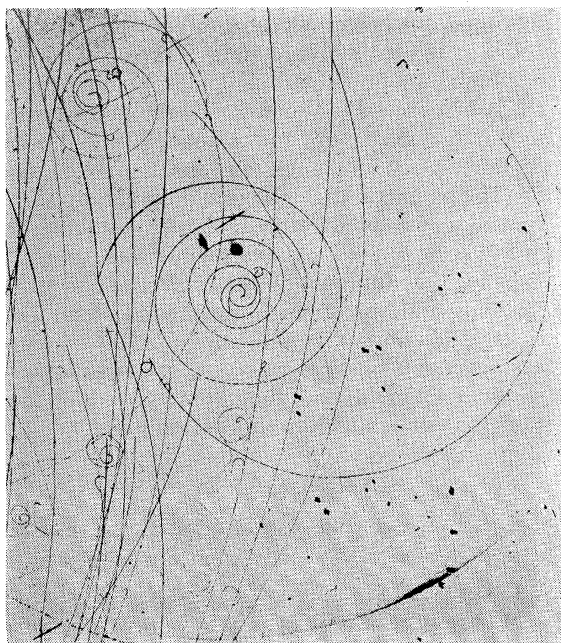


FIG. 1. Photograph of a typical internal pair.

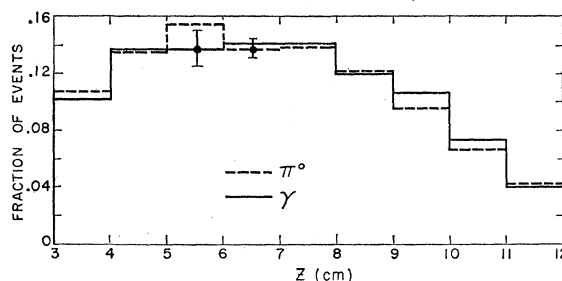


FIG. 2. Depth distribution of accepted events.

Among the other quantities calculated were the direction cosines of each track, the position of the vertex in the chamber, the net vector momentum of the pairs, the energy of the pair, the cosine of the angle between the electron and positron, a multiple scattering error,  $\Delta P/P$ , as given by

$$\Delta P/P = K/(\beta \cos \alpha \sqrt{l}),$$

where  $\alpha$  = dip angle,  $\beta = v/c$ ,  $l$  = length of track in cm,  $K = 0.29$  for  $H = 5.5$  kgauss,  $K = 0.18$  for  $H = 8.8$  kgauss, and the quantities  $y$  and  $x^2$  (to be defined later), which are pertinent to the theoretical calculations. The momentum of each track was corrected for ionization loss,  $0.219$  (MeV/c)/cm as determined by measurements on electron spirals which stopped in the chamber; and radiation loss,  $0.000815P$  (MeV/c)/cm which corresponds to a radiation length of  $72.5$  g/cm<sup>2</sup>.

In order to further insure adequate measurements, two more criteria were applied. The first was to restrict the depth position of the vertex away from the front and back glass windows so that only events whose vertex occurred at least 3 cm from these windows were accepted. Figure 2 shows the distribution of the events in depth ( $Z$ ). Any track which travels parallel to the magnetic field does not bend and therefore yields no information on its momentum. To eliminate these events a dip criterion was applied. Since the direction of the momentum of the electron-positron pair should be isotropic, the restriction of using only events whose  $Z$  direction cosine of the vector momentum ( $Z$  being along the magnetic field) was less than 0.8 introduced no bias. Figure 3 is a graph of the dip distribution. Both figures, 2 and 3, illustrate the similarity of the distributions for the pairs from  $n + \pi^0$  and  $n + \gamma$  reactions. These two further criteria reduced the number of events from 7000 to 4200.

#### V. ANALYSIS

Since the radiative capture reaction (B) is a two-body process, the  $\gamma$  ray is monoenergetic with the value of its energy  $E = 129$  MeV and momentum  $P = 129$  MeV/c. If one makes a plot of momentum vs energy (see Fig. 4), this  $\gamma$  ray would correspond to point  $a$ . But when this  $\gamma$  ray internally converts (since now the reaction product consists of three particles) the energy

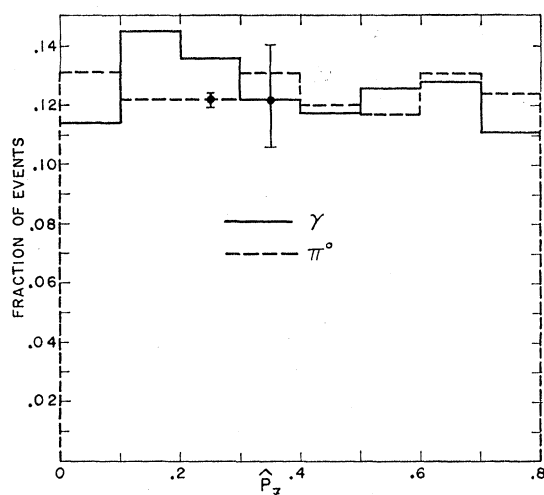


FIG. 3. Dip distribution of accepted events.

and momentum of the pair can lie anywhere along the line from  $a$  to its intersection with the  $E$  axis. Similar arguments can be made for the charge exchange reaction, (A). As is well known, the Lorentz transformation of the monoenergetic  $\gamma$  rays from the center of mass of the  $\pi^0$  to the laboratory system gives a distribution with  $55 < E_\gamma < 82$  Mev, and  $55 < P_\gamma < 82$  Mev/c. This is indicated by the  $45^\circ$  line in Fig. 4. When one of these  $\gamma$  rays is internally converted, the kinematically allowed momentum-energy region is changed from a line to an area as is indicated. The separation of events into the two categories, (A) and (B), consisted of plotting the energy and momentum of each event with its errors (i.e., multiple scattering, magnetic field drift, etc.) and designating as  $(n+\gamma)$  those events that fell along the indicated line or  $(n+\pi^0)$  those that appeared in the boxed-in region. In this manner, the 4200 events were apportioned; 1090 as due to  $(n+\gamma)$ ; 3065 as  $(n+\pi^0)$ ; and 44 events which were not distinguishable due to the fact that they fell in the overlapping region or that their nominal values fell in between the two regions but had large errors so that they overlapped both regions. In order to correctly apportion these 44 events, a histogram plot of the total energy of all the internal pairs was made, as is shown in Fig. 5. The accompanying smooth curve is the theoretically expected distribution as extracted from Kroll and Wada with a 7% experimental distribution folded in. This experimental resolution was determined by the shape of the 129-Mev peak which is very closely Gaussian. This resulted in putting 38 events into the  $(n+\gamma)$  category and designating 6 as due to  $(n+\pi^0)$ .

The following possible sources of background were considered:

(1)  $\pi^- + p \rightarrow n + \gamma + \gamma$ , with one of the  $\gamma$  rays being internally converted. Its rate, as compared to the internal conversion from the  $(n+\gamma)$  reaction, should be down a factor of  $\alpha$  due to the ratio of matrix elements,

and a factor of  $1/40$  from the ratio of their phase spaces. This would yield  $0.025\alpha \times 10^3 = \frac{1}{2}$  event. (The order-of-magnitude calculation for this reaction agrees with a precise value given by Joseph.<sup>9</sup>)

(2)  $\pi^- + p \rightarrow n + \pi^0 + \gamma$ , where one of the  $\gamma$  rays from the  $\pi^0$  is converted. In this reaction, the maximum energy of the low-energy  $\gamma$  ray is 3.2 Mev. As above, this rate should be reduced a factor of  $\alpha$  from matrix element considerations and  $< 1/40$  due to the ratio of phase spaces. This would yield a background of  $< 0.025\alpha \times 3 \times 10^3 = \frac{3}{2}$  events.

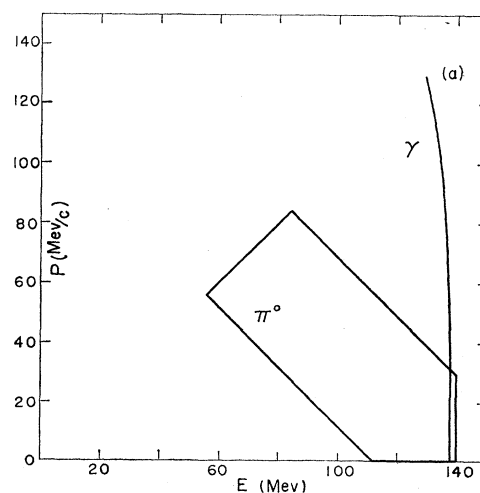
(3)  $\pi^- + p \rightarrow n + \pi^0$  in flight. The cross section for this reaction at these low energies is of the order of 8 mb.<sup>12</sup> The  $\pi^-$  flux in these pictures was  $4.26 \times 10^5$  (see Sec. VI) which would yield  $\sim 0.1$  event.

(4)  $\pi^- + p \rightarrow n + \gamma$  in flight. Since this cross section is  $< 1$  mb, it can be neglected.

(5) An external  $\gamma$  ray which is converted within 1 mm of the vertex. The cross sections for pair production by a  $\gamma$  ray at these energies, from a nucleus or an electron, are the same and equal to  $\sim 5$  mb. This would yield  $\sim 8$  events of each type. Most of the conversions from the electrons should appear as triplets. This agrees quite well with experience since 9 such events were observed. The nuclear recoil in pair production from a nucleon would be too low to allow a visible track in liquid hydrogen; therefore,  $\sim 8$  events have been included as internal pairs that were actually external pairs. This number was subtracted from both categories according to the ratio expected, five deducted from  $n+\pi^0$  events and three from  $n+\gamma$ .

(6)  $\pi^0 \rightarrow e^+ + e^-$ . Its calculated rate is down<sup>13,14</sup>  $\sim 10^{-7}$  from  $\pi^0 \rightarrow 2\gamma$ , and thus its effect vanishes.

The contamination from all these possible sources was, therefore, negligible.


 FIG. 4. Separation graph showing  $n+\pi^0$  region and  $n+\gamma$  line plotted as a function of the pair energy and momentum.

<sup>12</sup> H. A. Bethe and F. de Hoffmann, *Mesons and Fields* (Row, Peterson and Company, White Plains, New York, 1956), Vol. II.

<sup>13</sup> S. Drell, *Nuovo cimento* 11, 693 (1959).

<sup>14</sup> R. Oehme, *Phys. Rev.* 111, 1430 (1958).

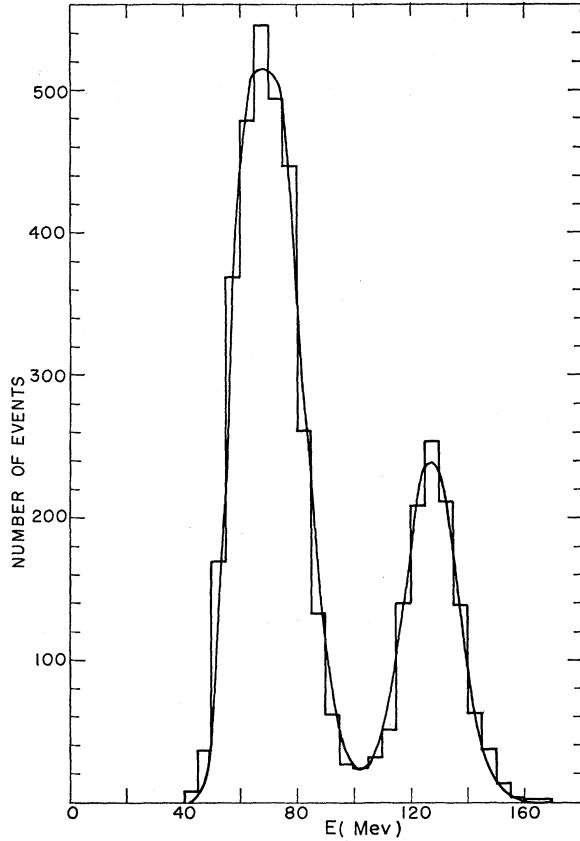


FIG. 5. Energy distribution of all the internally converted pairs. The histogram refers to the experimental data and the smooth curve to the theoretical fit.

## VI. RESULTS

The dynamic correlations of the internal conversion process are determined mainly by quantum electrodynamics and only weakly dependent upon meson theory—the strong interactions yielding at most a 2% correction. The distribution functions used to describe the electron-positron pair correlations are usually given in terms of two independent quantities:

$$x^2 = (E_+ + E_-)^2 - |\mathbf{P}_+ + \mathbf{P}_-|^2,$$

the virtual mass and

$$y = |E_+ - E_-| / |\mathbf{P}_+ + \mathbf{P}_-|,$$

the energy partition. Figures 6 and 7 are the differential distributions in  $x/\mu$  for the 3071  $\pi^0$  Dalitz pairs and for the 1128 internal pairs from the  $n + \gamma$  reaction. In the former case,  $\mu$  is the  $\pi^0$  rest mass, and in the latter is equal to  $(m_p + m_{\pi^-} - m_n) = 138.1$  Mev. The smooth curves are the theoretical predictions of Joseph, which include all electromagnetic corrections to first order in  $\alpha$ . The points correspond to the experimental data, the errors being the statistical error as determined by the number of events in each interval. Agreement seems quite good in both cases. The distribution function for

the  $\pi^0$  case is of the form,

$$f(x/\mu) = \Gamma^2(x/\mu) [(1 - x^2/\mu^2)^3 \times (1 - 4m^2/x^2)^{1/2} (1 + 2m^2/x^2)] (1/x),$$

where  $\Gamma(x/\mu)$  is the form factor for the  $\pi^0 \rightarrow 2\gamma$  vertex and is dependent on the strong interactions. In the calculations of Kroll and Wada and Joseph, the form factor was set equal to 1 since the distribution was strongly peaked at small  $x^2/\mu^2$  and thus deviations of  $\Gamma$  from 1 were expected to be small. Recently Berman and Geffen<sup>10</sup> have shown that a deviation of this form factor from 1 may be expected even though the energy transfer is relatively small,  $x_{\max}^2 = \mu^2$ . In order to investigate this possibility, they expanded the  $\Gamma(x/\mu)$  function keeping the first two terms:

$$\Gamma(x/\mu) = 1 + ax^2/\mu^2.$$

The effect of the term proportional to  $a$  increases for larger  $x^2/\mu^2$ , but the number of such events is small. Owing to these two effects, the greatest sensitivity to the parameter  $a$  was achieved by examining  $R$ , as defined below, in the regions

$$0.1 < x^2/\mu^2 < 1.0 \quad \text{and} \quad 4m^2/\mu^2 < x^2/\mu^2 < 0.1,$$

$$R \equiv \frac{\int_{0.1}^{1.0} f(x/\mu) d(x/\mu)}{\int_{4m^2/\mu^2}^{0.1} f(x/\mu) d(x/\mu)} = 0.108[1 + 0.409a].$$

The experimental value for  $R$  was  $272/2799 = (9.71$

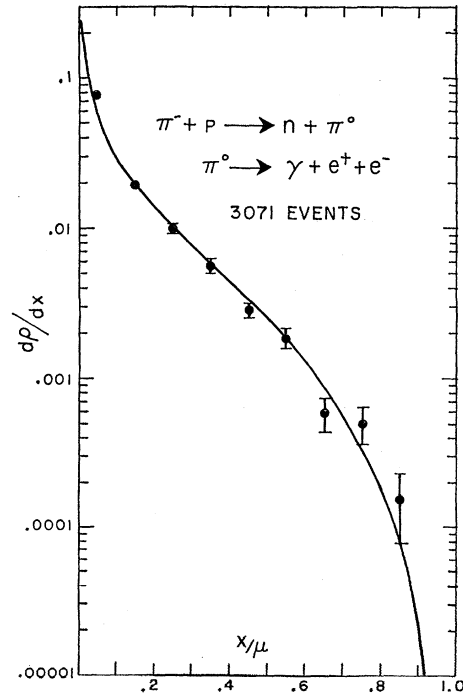


FIG. 6. Differential distribution in  $x/\mu$  (the virtual mass) for the internal pairs from  $n + \pi^0$  reaction.

$\pm 0.59) \times 10^{-2}$  which yields a value,  $a = -0.24 \pm 0.16$ . The error includes 0.12 due to statistics and 0.04 as an estimate of systematic effects due to the apportionment of the 44 ambiguous cases. The value of  $a$  expected from the calculations of Geffen and Berman on the basis of two-pion intermediate states in the process  $\pi^0 \rightarrow 2\gamma$  is of the order of  $+0.06$ . The experimental value is two standard deviations from this value and clearly inconsistent with a large positive value of  $a$ . (The number of additional events in the 0.1–1.0 category needed to yield a null value for  $a$  is of the order of 25.)

Figures 8 and 9 are the differential distributions in  $y$  for the  $(n+\pi^0)$  and the  $(n+\gamma)$  categories. The theoretical distributions are in the center-of-mass system of the  $\pi^0$  and the  $(n+\gamma)$  system, respectively. For the latter case, the laboratory and center-of-mass system coincide but for the  $\pi^0$ , the theoretical distribution should be transformed to the laboratory system before comparison with the experimental results. This transformation was performed for low  $y$  values and led to a negligible change from the center-of-mass values. It was not possible to do this for large  $y$  but since the transformation velocity,  $\beta=0.2$ , was so small and most of the pairs had small included angles, this effect is estimated to be small. Agreement seems reasonably good except for the highest  $y$  point in the  $\pi^0$  distribution

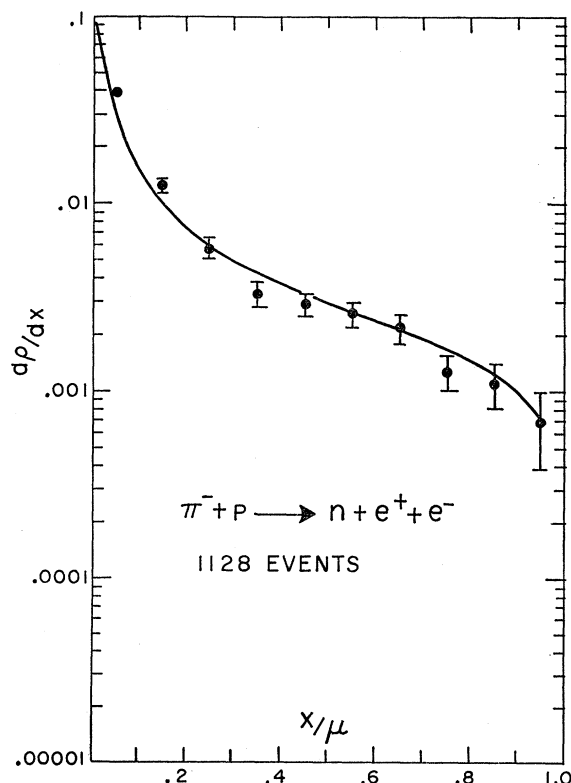


FIG. 7. Differential distribution in  $x/\mu$  (the virtual mass) for internal pairs from  $n+\gamma$  reaction.

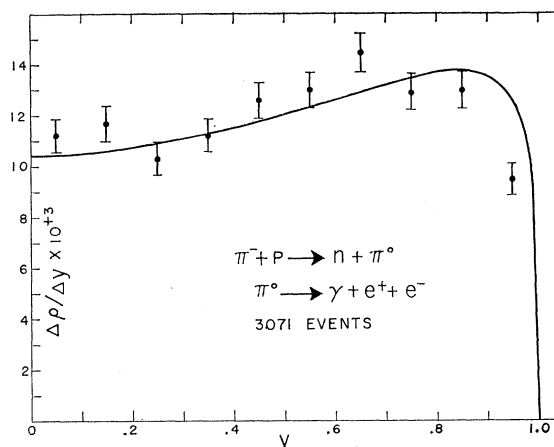


FIG. 8. Differential distribution in  $y$  (the energy partition) for internal pairs from  $n+\pi^0$  reaction.

which appears slightly low. The possibility was investigated that there were events where one of the tracks had  $\sim 0$  energy and was therefore missed. This was done by noting events where the  $\pi^-$  stops and a positron emerges from its vertex. There were three such events. Since the distribution in  $y$  is symmetric with respect to positron and electron, there should be  $\sim 3$  events with the reverse situation. This small correction was included in the 3071 events. The  $y$  distribution for the  $(n+\gamma)$  reaction agrees quite well with the theoretical expectations. The area under both curves has been normalized to  $\rho_{\pi^0}$  and  $\rho_\gamma$ , the internal conversion coefficients. (In a similar experiment but with the order of one-third the events,<sup>15</sup> experimental agreement with the theoretical prediction in  $x/\mu$  and  $y$  was also obtained.)

It has recently been pointed out by Joseph<sup>9</sup> that in the reaction  $\pi^- + p \rightarrow n + e^+ + e^-$ , the virtual  $\gamma$  ray has a longitudinal as well as transverse component. The same is not true for the  $\pi^0$  case, since in this latter instance the recoiling real  $\gamma$  ray is entirely transverse and must carry off one unit of angular momentum in its direction of motion. The distribution expected for the parameter  $y$  is markedly different for the two cases, independent of  $x/\mu$ . For the transversely polarized case, the distribution should be of the form  $(1+y^2)$ ; while for the longitudinal, it should be  $(1-y^2)$ . Unfortunately, the total contribution of the longitudinal part, as calculated, is only 2% of the total, but all of this occurs in the region of large virtual mass, i.e., large  $x^2/\mu^2$ . In fact, for  $x^2/\mu^2 > 0.16$ , the contribution should be 10% of the total. Experimentally, 170 events fell into this region. These events were fit to the function:

$$f(b, y^2) = K \{1 + (2b-1)y^2\},$$

where  $b$  is the % contribution of the transverse polarization and  $K$  is a normalization factor. This function has the property that when  $b=+1$  the contribution is

<sup>15</sup> M. Derrick *et al.*, Phys. Rev. **120**, 1022 (1960).

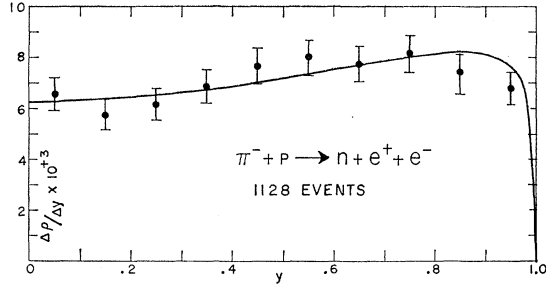


FIG. 9. Differential distribution in  $y$  (the energy partition) for internal pairs from  $n+\gamma$  reaction.

totally transverse, and when  $b=0$  it is entirely longitudinal. Since the events were so few, a maximum likelihood calculation was performed, where the likelihood  $L$  is given by

$$L = \prod_{i=1}^{170} f(b, y_i^2).$$

Figure 10 is a plot of the likelihood function as a function of  $b$ . The most likely value is  $\langle b \rangle = +0.70 \pm 0.20$ , the error corresponding to the half-maximum point. A least-squares fit to the data gave a similar result. This value of  $b$  agrees with the expected 10% for the longitudinal contribution, but the error is so large that it is also only  $1\frac{1}{2}$  standard deviations from zero. A factor of seven reduction in the error (or 50 times the number of single pairs) would be required to give a conclusive result.

The internal conversion coefficients for the two considered processes are related to the Panofsky ratio,  $\mathcal{P}$ , in the following manner:

$$\rho_{\pi^0} = \frac{(1+\mathcal{P}) N_{\pi^0}}{\mathcal{P} N}, \quad \rho_{\gamma} = (1+\mathcal{P}) \frac{N_{\gamma}}{N},$$

where  $N_{\gamma}$ ,  $N_{\pi^0}$  are the number of internal pairs from  $n+\gamma$  and  $n+\pi^0$  reactions, respectively;  $\rho_{\pi^0}$  and  $\rho_{\gamma}$  are the internal conversion coefficients for the two processes; and  $N$  is the number of  $\pi^-$ 's that could have produced these reactions. There are three quantities of interest: namely,  $\rho_{\gamma}$ ,  $\rho_{\pi^0}$ , and  $\mathcal{P}$ , but only two independent relations between them.

In the present experiment, the value for  $N$  was determined by counting the number of  $\pi^-$  stopping tracks in the fiducial region for a sample of pictures distributed throughout the run, as well as counting the total number of pictures. This number was corrected for the depth and dip restrictions by measuring the depth distribution of these counted beam tracks and using the dip distribution of the accepted pair events. This resulted in  $N = (4.26 \pm 0.14) \times 10^5$  tracks. In a previous publication,<sup>16</sup> a value of  $\mathcal{P} = 1.62 \pm 0.06$  was determined using the theoretical values for the ratio  $\rho_{\gamma}/\rho_{\pi^0}$  and the experimental values for  $N_{\pi^0}$  and  $N_{\gamma}$ .

<sup>16</sup> N. P. Samios, Phys. Rev. Letters 4, 470 (1960).

If one now accepts the theoretical ratio  $\rho_{\gamma}/\rho_{\pi^0} = 0.594$ ,<sup>9</sup> and the experimental quantities  $N_{\gamma}$ ,  $N_{\pi^0}$ , and  $N$  outlined above, then with this third relationship one can obtain individual values for  $\rho_{\gamma}$ ,  $\rho_{\pi^0}$  as well as the aforementioned value for  $\mathcal{P}$ . This serves as a consistency check on the data. Therefore:

$$\mathcal{P} = \frac{\rho_{\gamma} N_{\pi^0}}{\rho_{\pi^0} N_{\gamma}} = 0.594 \frac{3066}{1125} = 1.62 \pm 0.06,$$

$$\rho_{\pi^0} = \frac{(1+\mathcal{P}) N_{\pi^0}}{\mathcal{P} N} = \frac{2.62}{1.62} \frac{3066}{4.26 \times 10^5} = 0.01166 \pm 0.00047,$$

and

$$\rho_{\gamma} = (1+\mathcal{P}) \frac{N_{\gamma}}{N} = 2.62 \frac{(1125)}{4.26 \times 10^5} = 0.00694 \pm 0.00031.$$

The theoretically predicted values with electromagnetic corrections included are  $\rho_{\pi^0} = 0.01196$  and  $\rho_{\gamma} = 0.00710$ .<sup>9</sup> The experimental results are in excellent agreement with these individual values for the conversion coefficients. Previous measurements of these quantities<sup>6,7</sup> also showed agreement but their errors were orders of magnitude larger than the present ones due to lack of events.

## VII. CONCLUSIONS

The distributions in the variables  $y$  and  $x/\mu$  agree with the quantum electrodynamic calculations. Furthermore, the values of  $\rho_{\gamma}$  and  $\rho_{\pi^0}$  are consistent with the

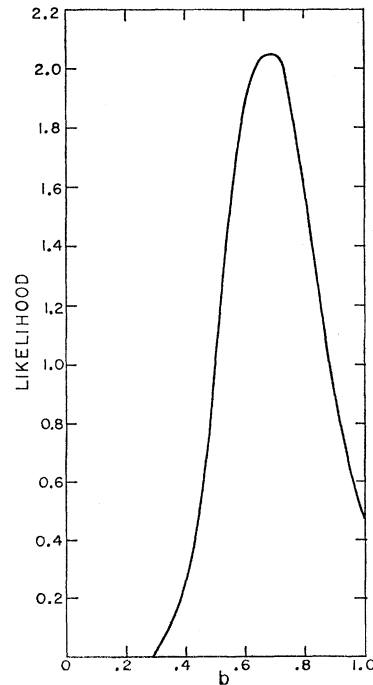


FIG. 10. Plot of likelihood function of  $b$  (mixing parameter for transverse and longitudinal polarizations) versus  $b$ .

theoretically predicted values, increasing the confidence in the experimental value of the Panofsky ratio,  $\rho = 1.62 \pm 0.06$ . It has been demonstrated that any investigation of the strong interaction in the  $\pi^0 \rightarrow 2\gamma$  process or any insight into the dynamics of virtual longitudinal gamma rays would require a sample of 5–50 times the present number of events.

In the  $\pi^0 \rightarrow 2\gamma$  case, the deviation of the form factor,  $\Gamma(x/\mu)$ , from unity was less than two standard deviations, the expansion parameter  $a$  being equal to  $-0.24 \pm 0.16$ . Recently it has been shown<sup>10,17</sup> that negative values of  $a$  can be obtained by including interference effects between  $2\pi$  and other intermediate states. In the case of virtual longitudinal  $\gamma$  rays in the  $n+\gamma$  reaction, the data yielded a result which was consistent with a small contribution as predicted by the calculations of Joseph. It is hoped that the present project will be continued because of these two latter interesting questions, but these present results were considered to be of sufficient interest to warrant publication now.

<sup>17</sup> H. S. Wong, Phys. Rev. (to be published).

# ACKNOWLEDGMENTS

I would like to thank the Columbia Bubble Chamber Group for aid in taking the pictures; especially Dr. R. Plano who was also mainly responsible for the design and construction of the measuring engines and Professor Jack Steinberger for his advice and encouragement during the progress of the experiment; Professor Norman Kroll for many useful discussions; Dr. Don Geffen for communicating his results prior to publication; Mr. Don Burd for programming the IBM 650 Computer; and Irene Garder, John Impeduglia, Dina Goursky, Alex Rytow, Hank Margosian, David Mauk, Alex Woskry, Galli Kaneletz, and Don McClure for finding and measuring these events. I also wish to acknowledge the help of Dr. Agnes Lecourtois who collaborated in the early phases of the work. Finally, this experiment would not have been conducted nor completed in such an orderly fashion without the aid of Miss Catherine MacLeod.

## $\Sigma^0 \rightarrow \Lambda^0 + e^+ + e^-$ and the $\Sigma^0 - \Lambda^0$ Relative Parity\*

NINA BYERS

*Institute of Theoretical Physics, Department of Physics, Stanford University, Stanford, California*

AND

HUGH BURKHARDT

*Department of Physics, California Institute of Technology, Pasadena, California*

(Received July 14, 1960)

The  $\Sigma^0 - \Lambda^0$  relative parity may be measured by observing correlation of polarizations in the process  $\Sigma^0 \rightarrow \Lambda^0 + \gamma$ . Internal conversion of the photon into an electron pair (Dalitz pair) serves as an analyzer which selects polarized photons. Theoretical results are presented which show that the Dalitz-pair decay mode of polarized  $\Sigma^0$ 's may be used to measure the  $\Sigma^0 - \Lambda^0$  relative parity.

**K**NOWLEDGE of the relative parity of the  $\Sigma^0$  and  $\Lambda^0$  hyperons would provide an important restriction on theoretical speculation about strong interactions. In this paper we wish to point out that there are correlations between the polarizations in the process

$$\Sigma^0 \rightarrow \Lambda^0 + \gamma, \quad (1)$$

that depend on the  $\Sigma^0 - \Lambda^0$  relative parity. The direct production of an electron pair by internal conversion serves as an analyzer for the photon polarization.

The form of the correlations can be seen from the following argument. Consider first the process (1)

where a real photon with momentum  $\mathbf{k}$ , electric vector  $\mathbf{E}$ , and magnetic vector  $\mathbf{B}$ , is emitted. Assuming that the  $\Sigma^0$  as well as the  $\Lambda^0$  has spin  $\frac{1}{2}$ , it follows from parity conservation, rotational and gauge invariance that, in the rest frame of the  $\Sigma^0$ , the  $S$  matrix in spin space has the form  $\boldsymbol{\sigma} \cdot \mathbf{B}$  or  $\boldsymbol{\sigma} \cdot \mathbf{E}$  according as to whether the  $\Sigma^0 - \Lambda^0$  parity is even or odd.<sup>1</sup> Since  $\boldsymbol{\sigma} \cdot \hat{n}$  is the spin rotation operator which rotates the spin through  $180^\circ$  about the  $\hat{n}$  direction, the spin of the  $\Lambda^0$  will be that of the  $\Sigma^0$  rotated through  $180^\circ$  about the direction of  $\mathbf{B}$  ( $\mathbf{E}$ ). Therefore, the  $\Lambda^0$ 's will be polarized if the  $\Sigma^0$ 's are polarized, and the expectation value  $\mathbf{P}_\Lambda$  of the  $\Lambda^0$  spin in its rest frame will be related to that of the  $\Sigma^0$ ,

\* Supported in part by the U. S. Atomic Energy Commission and by the U. S. Air Force through the Air Force Office of Scientific Research.

<sup>1</sup> Throughout this paper the first, or upper, of two alternatives refers to the case of even  $\Sigma^0 - \Lambda^0$  relative parity, and the other to odd.

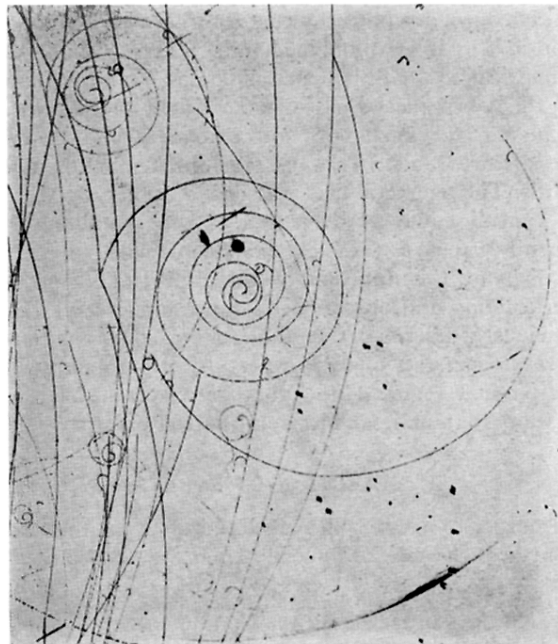


FIG. 1. Photograph of a typical internal pair.